Journal of Power Sources 581 (2023) 233480

Contents lists available at ScienceDirect

Journal of Power Sources

journal homepage: www.elsevier.com/locate/jpowsour

An in-depth investigation into the influence of temperature on the electrochemical behavior of electric double-layer capacitors containing ethyl isopropyl sulfone-based electrolytes

Lukas Köps, Fabian Alexander Kreth, Michel Klein, Andrea Balducci *

Friedrich-Schiller-University Jena, Institute for Technical Chemistry and Environmental Chemistry and Center for Energy and Environmental Chemistry Jena (CEEC Jena), Philosophenweg 7a, 07743, Jena, Germany

HIGHLIGHTS

- Ethyl isopropyl sulfone-based EDLCs display high performance at high temperature.
- The performance of acetonitrile-based EDLCs decrease at high temperature.
- Understanding the temperature-dependent behavior of supercapacitors.

ARTICLE INFO

Keywords:
Acetonitrile
Ethyl isopropyl sulfone
Electric double-layer capacitor
High temperature
Temperature dynamic

ABSTRACT

The surrounding temperature significantly impacts the electrochemical behavior of electric double-layer capacitors during operation. While low temperatures restrict the transport properties of the charge carriers and lower the overall cell performance, higher temperatures improve the transport properties and performance but lead to the decomposition of the materials. To address this issue, the supercapacitor's nominal voltage must be lowered to ensure a long cycle life. With the aim of understanding the temperature-dependent behavior of supercapacitors based on ethyl isopropyl sulfone and acetonitrile, various electrochemical investigations at different temperatures up to 80 °C are presented. Interestingly, these investigations reveal a contradictory performance evolution over the temperature caused by the different solvents. Supported by the different stabilities of these two electrolytes, different optimal temperature ranges of application for electric double-layer capacitors based on these solvents can be concluded from these findings.

1. Introduction

Energy storage devices such as batteries or supercapacitors have become essential for our life and are used in many applications related to key sectors such as transportation, renewable energy, and consumer electronics [1–4]. Due to the variety of applications, the requirements for these energy storage devices can be highly diverse. Properties such as energy density, power density, cycle life, and safety are decisive in the selection of the most suitable energy storage technology for a particular application [5]. Furthermore, energy storage devices must be able to work under a broad range of temperatures, different levels of humidity, and exposure to vibration and shock [6–8]. Therefore, the development of energy storage devices meeting these criteria is a major challenge.

Electric double-layer capacitors (EDLCs) are nowadays considered the devices of choice for high-power applications [9–11]. Many efforts are currently dedicated to improving the energy density of these devices and, at the same time, to extend their temperature range of use toward higher temperatures, e.g., above 60 °C [12–15]. To achieve this goal, the development of innovative electrolytes is fundamental. The utilized materials and surrounding temperature highly impact the charge storage mechanism of EDLCs [16–18]. As higher temperatures increase ion movement and transport properties in general, the reversible adsorption of ions at the interphase between electrode and electrolyte is accelerated. Thus, the charge storage by the formation of a double-layer is promoted, resulting in improved performance. At the same time, the electrolyte is more likely to decompose, leading to decreased stability and shorter cycle life [19–21]. At lower temperatures, the movement of ions is restricted, limiting the transport properties of the electrolyte.

* Corresponding author.
E-mail address: andrea.balducci@uni-jena.de (A. Balducci).

https://doi.org/10.1016/j.jpowsour.2023.233480
Received 17 April 2023; Received in revised form 12 July 2023; Accepted 1 August 2023
Available online 11 August 2023

These effects strongly depend on the physicochemical and thermal properties of the electrolyte solvent, such as viscosity, melting, and boiling point. Thus, a system operating well at low or moderate temperatures does not necessarily have to operate well at high temperatures and vice versa.

Currently, commercially available EDLCs contain acetonitrile (ACN) as the electrolyte solvent since its use makes possible the realization of electrolytic solutions with high ionic conductivity, low viscosity, and, thus, fast charge-storing processes, and high power densities [22–24]. However, the temperature and voltage ranges of ACN-based EDLCs are limited due to ACN's relatively low boiling point of 81.6 °C and electrochemical decomposition at cell voltages of 3.0 V or higher [25]. These characteristics limit the energy density as well as the stability at high temperatures of EDLCs. For this reason, several alternative electrolytes have been proposed and investigated in the last years [26–29].

Among the alternative organic solvents, sulfones exhibit one of the highest electrochemical stabilities due to the chemical stability of the sulfonyl group. In the past, Chiba et al. demonstrated the promising properties of electrolytes based on ethyl isopropyl sulfone (EiPS) for EDLCs [30,31]. Although EiPS-based electrolytes are known for their high stability, EiPS shows higher viscosity and, thus, inferior transport properties than state-of-the-art electrolytes based on ACN. This limits the high-power capabilities of this alternative class of electrolytes and causes higher internal resistance in the ELDCs containing this solvent, especially at low to moderate temperatures. However, our group has recently shown that when utilized at high temperatures (60–80 °C), the performance of EiPS-based EDLCs improves significantly and becomes even superior to that of devices containing the state-of-the-art electrolyte [32]. These results indicated that the use of EiPS-based electrolytes could be an effective strategy for the realization of EDLCs operating at high temperatures (60–80 °C), which are particularly challenging for conventional devices. However, further modification of the electrolyte is needed to reduce the resistance of devices based on EiPS and, at the same time, their electrochemical behavior at high temperatures must be understood in detail.

With the aim to gain information about these important points, in this study, we investigate in detail the behavior of EiPS-based EDLCs at different temperatures. The study utilized electrolytic solutions containing EiPS and the salts tetraethylammonium tetrafluoroborate ($TEABF_4$) and *N,N*-dimethylpyrrolidinium tetrafluoroborate ($Pyr_{11}BF_4$) [33,34]. The electrochemical behavior of the devices containing these alternative electrolytes has been compared to that of devices containing the 1 M $Pyr_{11}BF_4$ in ACN. This latter electrolyte has been selected since it shows higher performance and stability than conventional electrolytes containing $TEABF_4$ [35]. The influence of the temperature on the internal resistance, capacitance, and energy of the investigated EDLCs operating between 20 and 80 °C has been considered in detail. This revealed a contradictory evolution of the electrochemical performance of the devices containing these two solvents. While the electrochemical performance of EDLCs based on ACN fades with increasing temperature, the properties of devices based on EiPS improve to ultimately become comparable to the reference system at 80 °C. Furthermore, the impact of EiPS on the stability and self-discharge of EDLCs at different temperatures has been analyzed. This highlights the remarkably high stability of 1 M $Pyr_{11}BF_4$ in EiPS at high temperatures and high voltages.

2. Experimental section

2.1. Electrolyte preparation

The solvent EiPS was supplied from E-Lyte Innovations GmbH with a purity of 99.3% and a water content of <5 ppm and was used as received. The solvent ACN was purchased from Sigma-Aldrich with a purity of 99.8% and dried by adding a molecular sieve with a molecular pore size of 3 Å (Chemiewerk Bad Köstritz). The salts $TEABF_4$ and $Pyr_{11}BF_4$ were supplied by IoLiTec, both with >99% purity. Both salts were dried for 24 h in a vacuum glass oven at 80 °C and 1×10^{-2} mbar before use. For the following reported electrochemical investigations, the electrolytes 0.5 M $TEABF_4$ in EiPS, 1 M $Pyr_{11}BF_4$ in EiPS, and 1 M $Pyr_{11}BF_4$ in ACN were used.

2.2. Physicochemical properties

To measure the ionic conductivity of the electrolytes, a conductivity cell was placed in a Binder MK 53 climatic chamber to adjust the temperature in a range between -30 – 80 °C and measured with a Modulab XM ECS potentiostat according to a procedure described before [36]. The electrolyte's viscosity was determined using an Anton-Paar MCR 102 rotational viscometer with an applied shear rate of 1000 s^{-1}. Following a procedure described before, 500 μL of electrolyte were used for the measurement in a temperature range between -30 – 80 °C for the EiPS-based electrolytes and -30 – 50 °C for the ACN-based electrolyte [36].

2.3. Cell preparation

The electrodes utilized for the electrochemical measurements were provided by Skeleton Technologies with a mass loading of 7.5 mg cm^{-2} and an electrode area of 1.13 cm^2. Before application, one side of the activated carbon coating from the double-sided coating was removed with ethanol to match the experimental setup described below.

Electrochemical measurements were carried out in Swagelok-type cells in a two-electrode setup. Two identical electrodes (symmetrical cell) were used and separated with a 520 μm Whatman glass fiber disk soaked with 120 μL of the respective electrolyte. The cells were assembled in an argon-filled LABmaster pro glove box by MBRAUN. The content of H_2O and O_2 inside the glove box was not exceeding 1 ppm.

2.4. Electrochemical measurements

Temperature-dependent potentiostatic impedance spectroscopy was carried out in a climatic chamber (Binder KB 53) in a temperature range of 20–80 °C. Fresh cells were conditioned with galvanostatic charge-discharge for 100 cycles with a current rate of 1 A g^{-1} in a voltage range of 0–2 V at 20 °C before impedance spectroscopy. Impedance spectra were recorded in a frequency range of 100 kHz–10 mHz with a BioLogic MPG-2 potentiostat starting at 20 °C. After each measurement, the temperature was increased by 1 °C before performing the following impedance spectroscopy resulting in a temperature staircase similar to the one shown in Fig. 1a.

Temperature-dependent galvanostatic charge-discharge was performed with a BioLogic MPG-2 potentiostat in the same climatic chamber in the same temperature range with a current rate of 1 A g^{-1} to derive the specific energy. In a voltage range between 0 and 2.7 V, the cells were cycled five times before increasing the upper voltage limit in steps of 50 mV. After each increase, another five cycles were performed until reaching a limit of 3.4 V. This protocol was repeated every 2 °C starting from 20 °C until reaching 80 °C (Fig. 1). The cells used were conditioned as the cells used for temperature-dependent impedance spectroscopy before the actual measurement.

The electrochemical stability window was measured at four different temperatures (20 °C, 40 °C, 60 °C, and 80 °C) using a Binder KB 53 climatic chamber. Linear sweep voltammetry (LSV) was employed at a scanning rate of 1 mV s^{-1} utilizing a Biologic MPG-2 potentiostat. To determine the respective anodic and cathodic electrochemical stability limits, separate LSV tests were conducted. These tests involved scanning from the open-circuit potential towards more positive potentials (anodic limit) or more negative potentials (cathodic limit). The working electrode consisted of a platinum electrode, while a self-standing oversized activated carbon electrode served as the counter electrode. As a quasi-reference electrode, an Ag wire was utilized.

The electrochemical stability of the electrolytes was investigated by

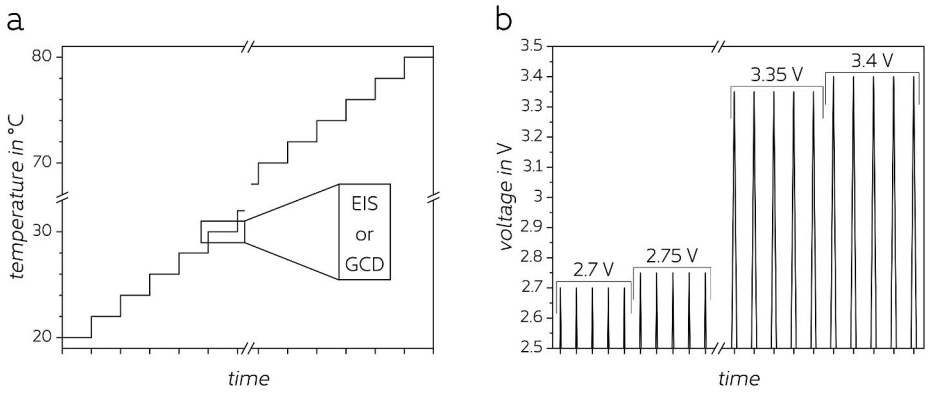

Fig. 1. Schematic illustration of a) the temperature staircase during temperature-dependent electrochemical impedance spectroscopy and galvanostatic charge-discharge measurements with temperature steps of 2 °C, and b) the charge-discharge protocol performed every 2 °C with 1 A g^{-1}. The voltage limit was increased by 50 mV starting from 2.7 V until reaching 3.4 V after 5 cycles were performed per voltage limit.

performing float tests at different voltages and temperatures for 500 h with an Arbin LBT21084 potentiostat. After assembling, the cells were conditioned as described before and placed in a Binder KB 53 climatic chamber for temperature adjustment. Every 20 h, five galvanostatic charge-discharge cycles were performed with a current rate of 1 A g^{-1} between 0 V and the applied float voltage to determine the specific capacitance of the cell.

Self-discharge measurements were performed with a BioLogic VMP-3 potentiostat at different temperatures in a Binder KB 53 climatic chamber. After holding the voltage constant at 3.0 V for 10 min–20 h, the self-discharge was measured by recording the open-circuit potential for 24 h. To avoid differences caused by the cell assembling, the same cells were used to measure the self-discharge at all temperatures, starting at 20 °C. Before the self-discharge measurements, the cells were conditioned as described before.

2.5. Electrochemical data evaluation

The capacitance C of the temperature-dependent impedance spectroscopy was calculated by

$$C = \frac{-1}{2\pi f Im(Z)}$$

with f being the frequency and $Im(Z)$ the imaginary quantity of the complex resistance. The presented time t corresponds to the reciprocal value of the applied frequency f, yielding $t = 1/f$. The showcased specific capacitance corresponds to the capacitance of the cell containing two electrodes.

The maximum energy E_{max} was calculated by integrating the discharge semi-period of the instantaneous power $p(t)$:

$$E_{max} = \int_{t_0}^{T} p(t)dt = \int_{t_0}^{T} v(t)i(t)dt$$

with t_0 being the initial time and T the final time of the discharge, $v(t)$ and $i(t)$ being the instantaneous voltage and current. The maximum power P_{max} corresponds to the maximum of the modulus function of $p(t)$.

The capacitance during float tests was determined for the last discharge cycle of the galvanostatic charge-discharge between each floating period. The linear extrapolation was performed utilizing the latter 90% of the voltage profile to exclude the initial voltage drop from the extrapolation. Finally,

$$C = \frac{I}{dV/dt}$$

yields the capacitance C with I being the applied current and dV/dt the resulting slope from extrapolation of voltage V over time t.

3. Results & Discussion

In order to understand the impact of the temperature on the resistance of EiPS-containing EDLCs, electrochemical impedance spectroscopy (EIS) was performed in these devices in their discharged state. During the measurement, the temperature was increased incrementally (in steps of 1 °C) from 20 to 80 °C. For comparison with the state-of-the-art electrolyte solvent, an EDLC based on 1 M $Pyr_{11}BF_4$ in ACN was investigated following the same procedure. As shown in Fig. 2, the Nyquist plots obtained from these temperature-dependent EIS measurements show that the systems containing 0.5 M $TEABF_4$ in EiPS (Fig. 2a) and that containing 1 M $Pyr_{11}BF_4$ in EiPS (Fig. 2b) display different behavior. While an increase in temperature strongly decreases the resistance of both devices, as indicated by the shift toward lower values on the real axis, the lower concentrated electrolyte based on $TEABF_4$ displays overall higher resistances. At the same time, an increase in temperature reduces the prominence of the Warburg impedance in both systems, highlighting the improved ion transport at higher temperatures. Compared to the EDLCs based on EiPS, the reference system containing ACN displays significantly lower resistances (Fig. 2c) and better transport properties as indicated by the less dominant Warburg impedance. However, in contrast to EiPS, the lower boiling point of ACN causes the systems' performance to begin to decrease at a temperature of ca. 55 °C, as indicated by the spectra shifting to higher resistance values. The different influences of EiPS and ACN on the cell resistances can be correlated to the physicochemical properties of the electrolytes (Fig. S1 in Supplementary Information (SI)). Finally, all spectra feature a capacitive tail at low frequencies whose height decreases with increasing temperature. Following equation (1) with C being the capacitance, f the frequency, and $Im(Z)$ the imaginary part of the complex resistance, the decrease of the imaginary quantity indicates an increase in capacitance.

$$C = \frac{-1}{2\pi f Im(Z)} \quad (1)$$

Thus, the maximum amount of energy that can be stored increases for both EDLCs according to equation (2):

$$E_{max} = {}^1\!/_2\, CV^2 \quad (2)$$

With E_{max} being the maximum energy and V being the cell voltage. However, it is important to note that EIS performed in the discharged state does not promote the electrochemical decomposition of the devices. Thus, a loss of capacitance or energy due to electrochemical degradation processes cannot be observed by EIS to an extent as with other techniques, such as galvanostatic charge-discharge (GCD). That means that this observation of increasing capacitance and energy is not necessarily true for cycling EDLCs galvanostatically while increasing the

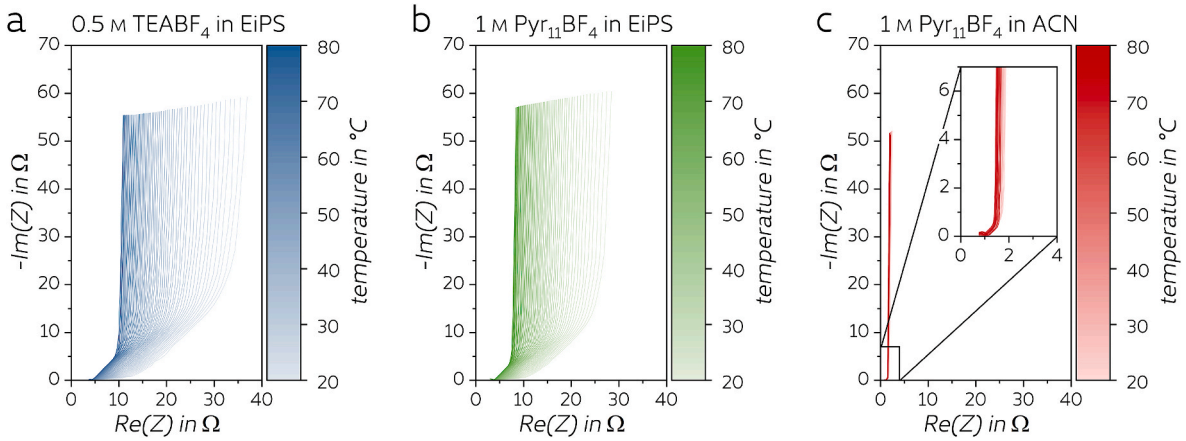

Fig. 2. Influence of the temperature on the impedance of symmetric EDLCs based on a) 0.5 M $TEABF_4$ in EiPS, b) 1 M $Pyr_{11}BF_4$ in EiPS, and c-d) 1 M $Pyr_{11}BF_4$ in ACN in a frequency range from 100 kHz–10 mHz and a temperature range from 20 to 80 °C with a temperature difference between each recorded impedance spectrum of 1 °C.

temperature since other effects might influence their performance.

In addition to the resistance, EIS can be used to gain information about the kinetics of the energy storage mechanism of an EDLC. When considering the semi-periodical signals of current and voltage during GCD comparable to the sinusoidal signals of current and voltage during EIS, the reciprocal value of the applied frequency during EIS – which is a time – can be treated as a charge-discharge time. Thus, this time represents the given timeframe for forming and dismantling the electric double-layers on the electrode surfaces. Although the charge storage process is relatively fast compared to other energy storage technologies, this process is not occurring instantaneously but requires a specific time depending on the properties of the utilized materials, such as pore and ion sizes, transport properties, and the nature of the solvent shell. Therefore, evaluating a particular system's limits is of great interest. To evaluate the quantity of this time limitation, the specific capacitance (equation (1)) can be correlated with the time or frequency, respectively. In this case, since the only component differentiating the devices is the electrolyte, this plot provides a clear indication of the influence of this component on the performance of the investigated EDLCs. As shown in Fig. 3, due to the limited transport properties of EiPS-based electrolytes, EDLCs containing EiPS as the electrolyte solvent show relatively low specific capacitance at 20 °C (Fig. 3a–b) and require longer times for the double-layer formation compared to the ACN-based EDLC (Fig. 3c). The much shorter time required to form high-capacitive double-layers in this latter device is clearly due to the superior transport properties of its electrolyte. When increasing the temperature, the charge storage process accelerates independently on the used electrolyte enabling higher achievable capacitance values at the same charge-discharge time.

In the case of the device containing 0.5 M $TEABF_4$ in EiPS, at a charge-discharge time of 20 s, the specific capacitance increases from 11 F g^{-1} at 20 °C to 16 F g^{-1} at 80 °C. In the same charging time, the EDLC based on 1 M $Pyr_{11}BF_4$ in EiPS achieves a specific capacitance of 12 F g^{-1} at 20 °C, increasing to 16 F g^{-1} at 80 °C. This increase in capacitance caused by the temperature is also significantly reducing the time needed to reach a specific capacitance value. For example, in the cases discussed above, an increase in temperature from 20 °C to 80 °C reduces the time needed to reach the maximum capacitance observed at the lower temperature by 75% (from 20 s to 5 s). As expected, the better transport properties and lower diffusion limitation of ACN enable much faster charge-discharge times (<1 s) compared to that possible in the EiPS-based devices. These results are clearly indicating that the nature of the solvent has a tremendous impact on the capacitance as well as on the time of charge-discharge of EDLCs.

Although of great importance, the capacitance, and the suitable timeframe for the charge-discharge of devices are not the only parameters of importance for the evaluation of a novel electrolyte. Also, the electrochemical stability is a property that needs to be carefully addressed as it strongly affects the stability of the devices at a defined cell voltage. For this reason, GCD measurements were performed to gain information about this important aspect. Since the stability of an EDLC strongly depends on the applied voltage, it is important to identify the impact of the voltage at a certain temperature on the characteristic parameters of the cell. A common way to describe the stability of a supercapacitor is to report the specific capacitance or capacitance retention. By giving detailed information about the charge storage capability in a certain voltage window, this parameter is suitable for tracking changes in the interaction of electrode material and electrolyte ions caused by degradation processes. However, important factors such as the resistivity of the utilized materials have only a minor influence on the capacitance since the capacitance should be constant over the operating voltage range in ideal EDLCs. Thus, a parameter giving a more comprehensive overview of the performance of an EDLC would be the specific energy since it includes the capacitance as well as the voltage, which is influenced by the cell resistance through overpotentials. It is essential to remark that the specific energy should not be computed by equation (2) in this case since this would exclude the influence of the resistance when inserting the applied upper voltage limit into the equation. Instead, the energy should be derived from the integration of the instantaneous power during GCD, which equals the product of the instantaneous current and voltage and, thus, considers the influence of the resistance. The voltage profiles of the three investigated electrolytes obtained from GCD are depicted exemplary for cell voltages of 2.7 V, 3.0 V, and 3.4 V in Fig. 4 and were recorded in a temperature range of 20–80 °C at a current density of 1 A g^{-1}. In general, all systems show the triangular behavior typical for EDLCs indicating a constant capacitance over the investigated voltage range. Thus, when increasing the cell voltages, the charge-discharge periods become longer. The voltage profiles highlight the dependency of the resistance on the temperature, as discussed for the impedance spectra before by the evolution of the ohmic drop. In the case of the EiPS-based electrolytes (Fig. 4a–b), the ohmic drops significantly decrease with increasing temperatures leading to higher exploitable voltage ranges. Thus, the duration of the full charge-discharge period increases. Since the measurement is performed with a constant current, the longer charge-discharge times indicate higher amounts of storable charges and, thus, higher energies at the same time. Furthermore, the difference in resistivity between the 0.5 M $TEABF_4$ in EiPS and 1 M $Pyr_{11}BF_4$ in EiPS becomes clear by this observation. While the EDLCs containing EiPS display improved performance at higher temperatures, the ACN-based device shows a contradictory behavior (Fig. 4c). The low resistance of the latter system increases with

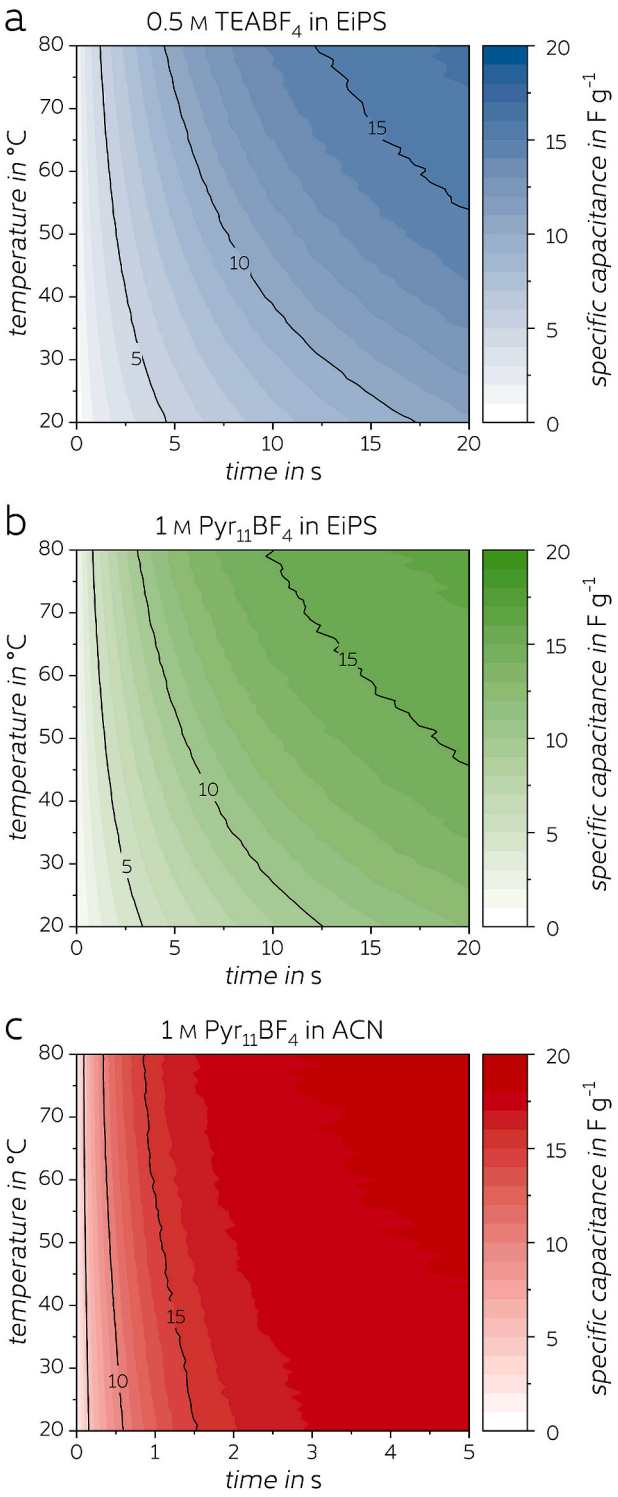

Fig. 3. Evolution of the specific capacitance of a symmetrical EDLC based on a) 0.5 M $TEABF_4$ in EiPS, b) 1 M $Pyr_{11}BF_4$ in EiPS, and c-d) 1 M $Pyr_{11}BF_4$ in ACN in a frequency range from 100 kHz–10 mHz and a temperature range from 20 to 80 °C with a temperature difference between each recorded impedance spectrum of 1 °C. The reciprocal quantity of the frequency corresponds to the shown time and indicates the charge-discharge time. The black contour lines show the development of the specific capacitance at the indicated values.

increasing temperature leading to shorter charge-discharge periods. Comparing the two systems containing $Pyr_{11}BF_4$, at 80 °C, the charge-discharge times become comparable, demonstrating a similar performance under these conditions.

Fig. 5 compares the specific energy of EDLCs based on the investigated electrolytes from the described GCD (carried out at 1 A g^{-1}) with different upper voltage limits in a range from 2.7 to 3.4 V. As shown, the variation of the quantity of the specific energy with the changing voltage and temperature are strongly affected by the electrolyte utilized in the devices. As expected, the ACN-based EDLC shows a higher energy storage capability over the investigated voltage and temperature ranges (specific energy of 45.1 Wh kg^{-1} and 36.9 Wh kg^{-1} at 20 °C and 80 °C, respectively). However, it is important to notice that these devices show a gradual decrease of specific energy with increasing temperature, highlighting the limited performance of ACN-based supercapacitors at elevated temperatures. This is not the case for the EiPS-based EDLCs, which continuously increase their energy density with the temperature and display a maximum at 80 °C independently of the cell voltage. However, it is important to observe that the selection of the conductive salt has a tremendous impact on the achievable specific energy. While the EDLC containing 0.5 M $TEABF_4$ in EiPS stores 21.6 Wh kg^{-1} at 80 °C and 3.4 V, that containing 1 M $Pyr_{11}BF_4$ in EiPS achieves 35.5 Wh kg^{-1} under the same conditions. The different trend observed between ACN and EiPS-based devices confirms that this latter solvent is particularly suited for applications at high temperatures. Based on these results from temperature-dependent EIS and GCD, the electrolyte 1 M $Pyr_{11}BF_4$ in EiPS was selected over 0.5 M $TEABF_4$ in EiPS for further investigation due to its more promising properties and higher specific power.

To further showcase the different development in the performance of EiPS-based and ACN-based electrolytes with increasing temperatures, Fig. 6a shows the temperature-dependent evolution of specific energy and maximum specific power of the investigated devices when tested at 1 A g^{-1}. Selecting 2.7 V, 3.0 V, and 3.4 V out of the investigated range of voltage limits shown before, each device shows the highest specific power at a voltage of 3.4 V. At the same time, the lowest power is observed at 2.7 V due to the applied constant current rate (1 A g^{-1}). The EiPS-based device significantly improves specific energy and maximum specific power when increasing the temperature to 80 °C. In contrast, the ACN-based electrolyte, which shows the highest specific energy and power, displays a contradictory trend as indicated by the arrows. With increasing temperature, the performance becomes worse. Furthermore, the temperature-dependent evolution of specific energy and power highlights the convergence of both pyrrolidinium salt-based systems in terms of performance at high temperatures. At 80 °C, the alternative electrolyte is thus quite comparable to the state-of-the-art. Fig. 6b shows the ragone plot of the considered pyrrolidinium-based electrolytes at different temperatures obtained by galvanostatic cycling at different current rates up to 3.0 V. As observed before, the EDLCs show contradictory trends in the evolution of their performance based on the utilized solvent. While the decrease in performance of the ACN-based device at high temperatures is relatively small, the improvement in performance of EDLCs containing EiPS is pronounced especially at higher current rates. Here, EiPS-based EDLCs benefit most from the improved transport properties when increasing the temperature. This highlights the possibilities of EiPS-based electrolytes at high temperatures for high-power applications.

The stability and lifetime of EDLCs under certain conditions can be investigated by float tests that keep the device in a charged state for a longer time. Performing float tests at different temperatures and voltages enables an estimation of their impact on the grade of degradation and its impact on the electrochemical performance. This extends the understanding of temperature-dependent stability gained from assessing the electrochemical stability window (Fig. S2 in the SI). From this becomes clear, that the voltage window shrinks for both electrolytes when increasing the temperature from 20 °C to 80 °C. Fig. 7 shows the evolution of the capacitance retention of EDLCs containing 1 M $Pyr_{11}BF_4$ in EiPS and ACN as electrolytes at different temperatures and floating voltages. At 20 °C (Fig. 7a), both systems display high stability against degradation and can be operated up to a voltage of 3.4 V without immediate failure. While the ACN-based electrolyte shows a faster aging

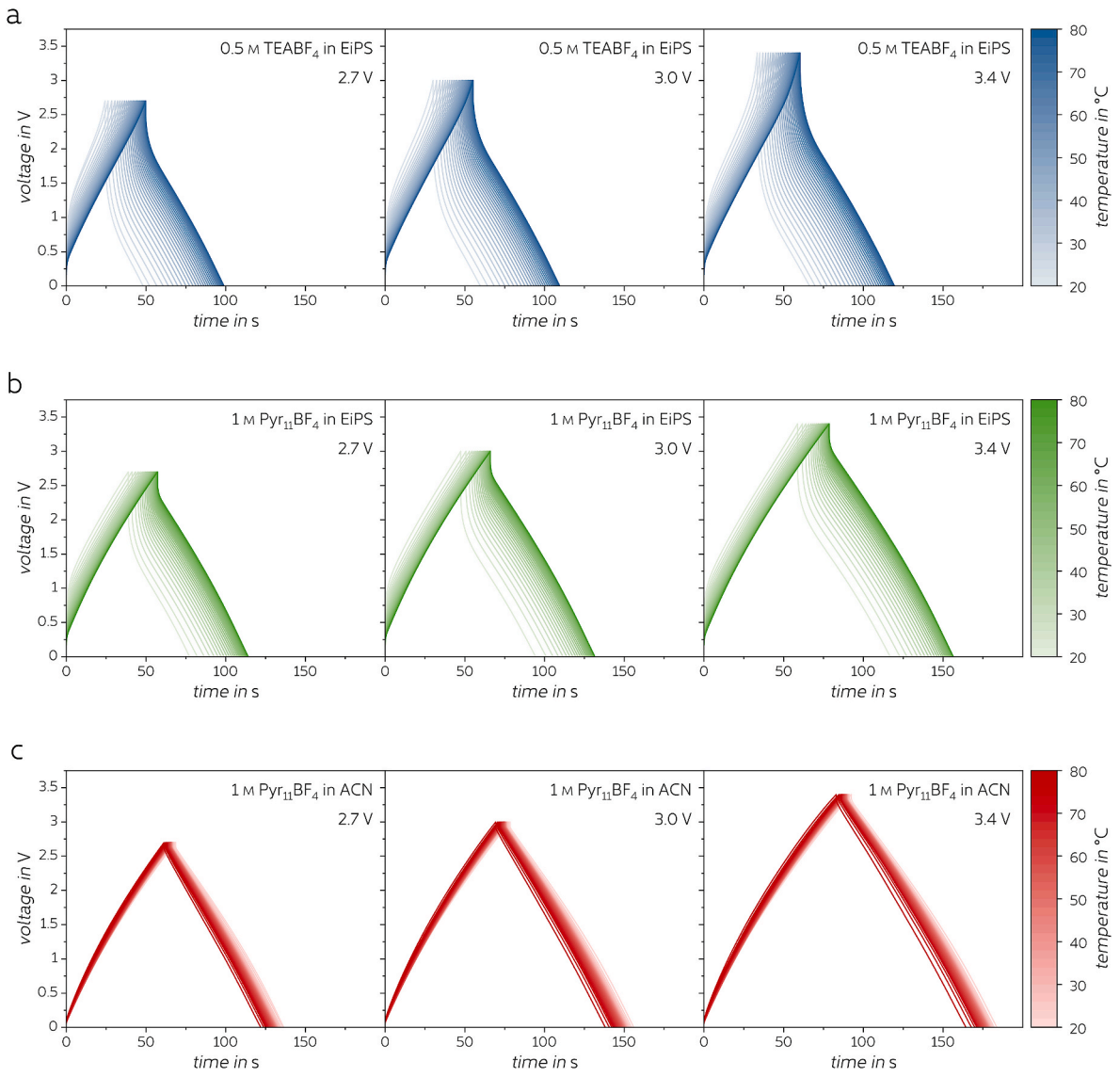

Fig. 4. Evolution of voltage profiles of symmetrical EDLCs containing a) 0.5 M $TEABF_4$ in EiPS, b) 1 M $Pyr_{11}BF_4$ in EiPS, and c) 1 M $Pyr_{11}BF_4$ in ACN at 2.7 V, 3.0 V, and 3.4 V. The profiles were recorded galvanostatically at a current rate of 1 A g^{-1} while gradually increasing the temperature in steps of 2 °C from 20 to 80 °C after cycling with incrementally increasing upper voltage limit.

process and retains 51% of its initial capacitance after 500 h, the EiPS-based electrolyte features a higher stability with a capacitance retention of 84%. When increasing the voltage to 3.6 V, the electrolyte based on ACN decomposes significantly at the beginning of the floating, causing a fast loss of capacitance with 57% of capacitance retention after 60 h. On the other hand, the alternative electrolyte based on EiPS still shows high stability under these conditions, displaying a capacitance retention of 77% after floating for 500 h. At an increased temperature of 60 °C, degradation processes are promoted due to the higher available energy. Thus, the operating voltage has to be reduced to operate the devices under stable conditions. As depicted in Fig. 7b, EiPS-based EDLCs show an initial decrease in capacitance retention after the first hours of floating, indicating the presence of decomposition reactions. However, the systems stabilize after this initial degradation indicating the formation of a passivation layer, as discussed in a previous work with 0.5 M $TEABF_4$ in EiPS as the electrolyte [32]. This initial degradation causes a loss in capacitance and, thus, a lower number of storable charges and energy but, once it is ended, it increases the system's long-term stability. Due to this behavior, the EDLCs based on EiPS display capacitance retentions of 79% at 3.2 V and 69% at 3.4 V, respectively, after floating for 500 h. In contrast, the devices based on ACN display no change in the speed of degradation and age faster with capacitance retentions of 51% after 300 h of floating at 3.2 V and 52% after 100 h of floating at 3.4 V. When increasing the temperature further to 80 °C, the aging of the devices accelerates further as well (Fig. 7c). Especially the ACN-based EDLCs suffer at this high temperature, which is close to the boiling point of the solvent (81.6 °C) [25]. Fast aging occurs, leading to capacitance retentions of 58% after floating for 60 h at 3.0 V and 19% after floating for 40 h at 3.2 V. The EDLCs based on EiPS show much higher stability at this temperature. As observed in the first hours of floating at 60 °C, also at 80 °C the capacitance decreases in the first floating period. While the degradation continues when floating at 3.2 V to reach a capacitance retention of 35% after 160 h, the EDLC stabilizes at a voltage of 3.0 V and features a capacitance retention of 72% after 500 h. These floating results highlight the interesting properties of EiPS-based electrolytes that show high stability under harsh conditions where electrolytes based on the state-of-the-art solvent ACN degrade. However, this stability comes with the price of losing energy storage capability to form a passivation layer that prevents the system from further degradation and a higher resistance compared to

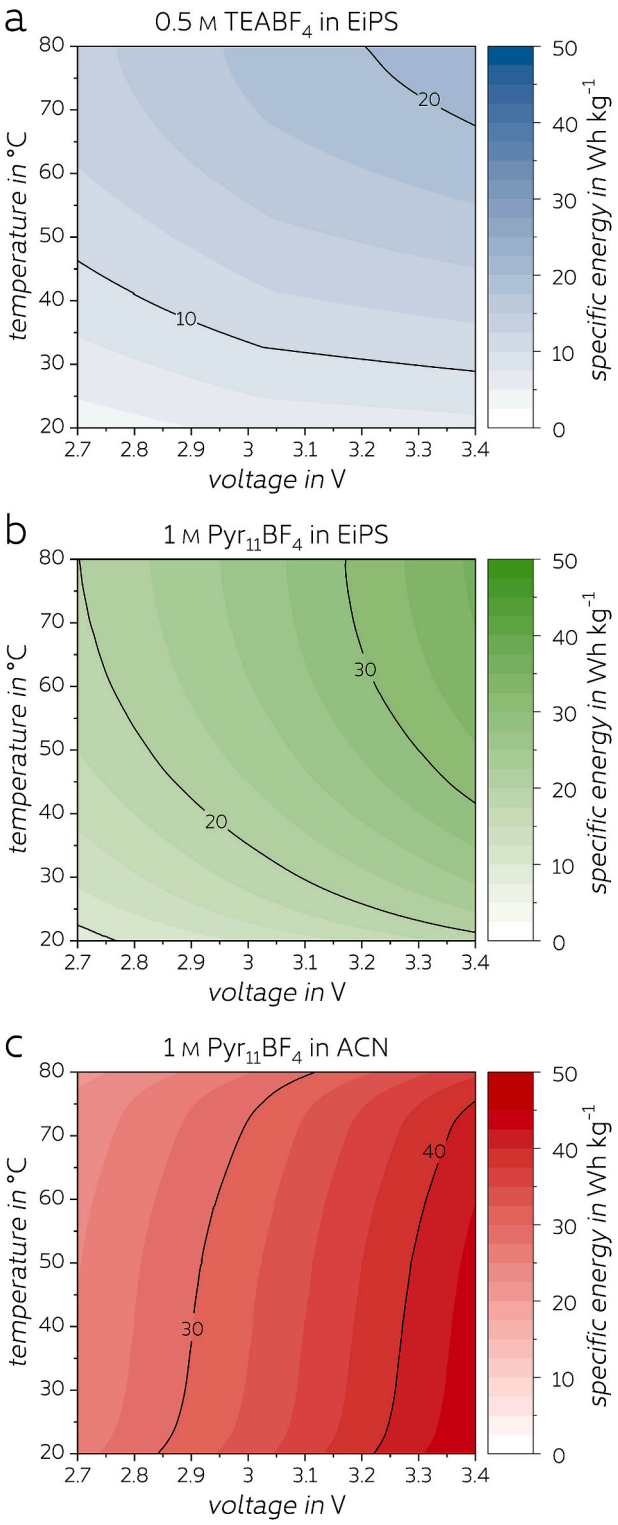

Fig. 5. Evolution of the specific energy of symmetrical EDLCs based on a) 0.5 M $TEABF_4$ in EiPS, b) 1 M $Pyr_{11}BF_4$ in EiPS, and c) 1 M $Pyr_{11}BF_4$ in ACN derived by GCD carried out at 1 A g^{-1} with increasing temperature in a range of 20–80 °C. The black contour lines show the development of the specific energy at the indicated values.

ACN-based electrolytes as discussed before.

Compared to other energy storage systems, such as batteries, supercapacitors suffer from relatively high self-discharge which is related to the underlying charge storage mechanisms. In addition, the intensity of the self-discharge strongly depends on the utilized electrode

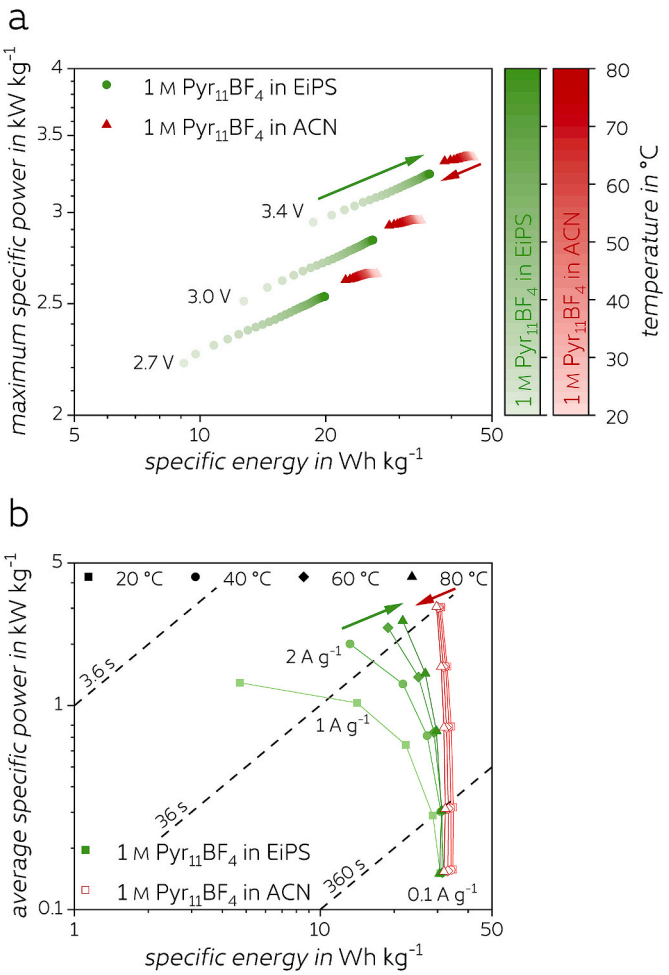

Fig. 6. a) Temperature-dependent evolution of the maximum specific power and specific energy of symmetrical EDLCs in a temperature range of 20–80 °C. The EDLCs based on the electrolytes 1 M $Pyr_{11}BF_4$ in EiPS and 1 M $Pyr_{11}BF_4$ in ACN were cycled galvanostatically with 1 A g^{-1} with increasing temperature. The upper voltage limits of 2.7 V, 3.0 V, and 3.4 V were selected as representatives. The arrows indicate the direction of performance evolution with increasing temperature. b) Ragone plot of symmetrical EDLCs containing 1 M $Pyr_{11}BF_4$ in EiPS and 1 M $Pyr_{11}BF_4$ in ACN at different temperatures and current rates when cycled galvanostatically to 3.0 V. The dashed lines represent the times required to fully (dis)charge the EDLCs at the respective current rates. The arrows indicate the direction of performance evolution with increasing temperature.

and electrolyte materials. To assess the influence of the considered electrolytes on the loss of stored energy during operation, self-discharge measurements were performed. For a better relation to the previous results on the stability, the measurements were conducted at three different temperatures, namely 20 °C, 60 °C, and 80 °C. Fig. 8 depicts the voltage retention after self-discharging EDLCs containing 1 M $Pyr_{11}BF_4$ in EiPS and 1 M $Pyr_{11}BF_4$ ACN as electrolytes for 24 h from a starting voltage of 3.0 V. At a temperature of 20 °C (Fig. 8a), both EDLCs show similar behavior when increasing the initial holding time before the self-discharge. However, the ACN-based system generally shows lower self-discharge compared to the EDLC based on EiPS. In addition, a longer holding time has a more beneficial effect on the former system, reducing the loss in voltage from 41% at a holding time of 10 min to 20% after holding for 20 h. On the other hand, the self-discharge of the EiPS-based EDLC is less affected by the holding time, showing an improvement from 57% of lost voltage to 47% when prolonging the holding time from 10 min to 20 h. The voltage profiles corresponding to the presented voltage retentions are shown in Fig. S3 of the SI. At increased temperatures,

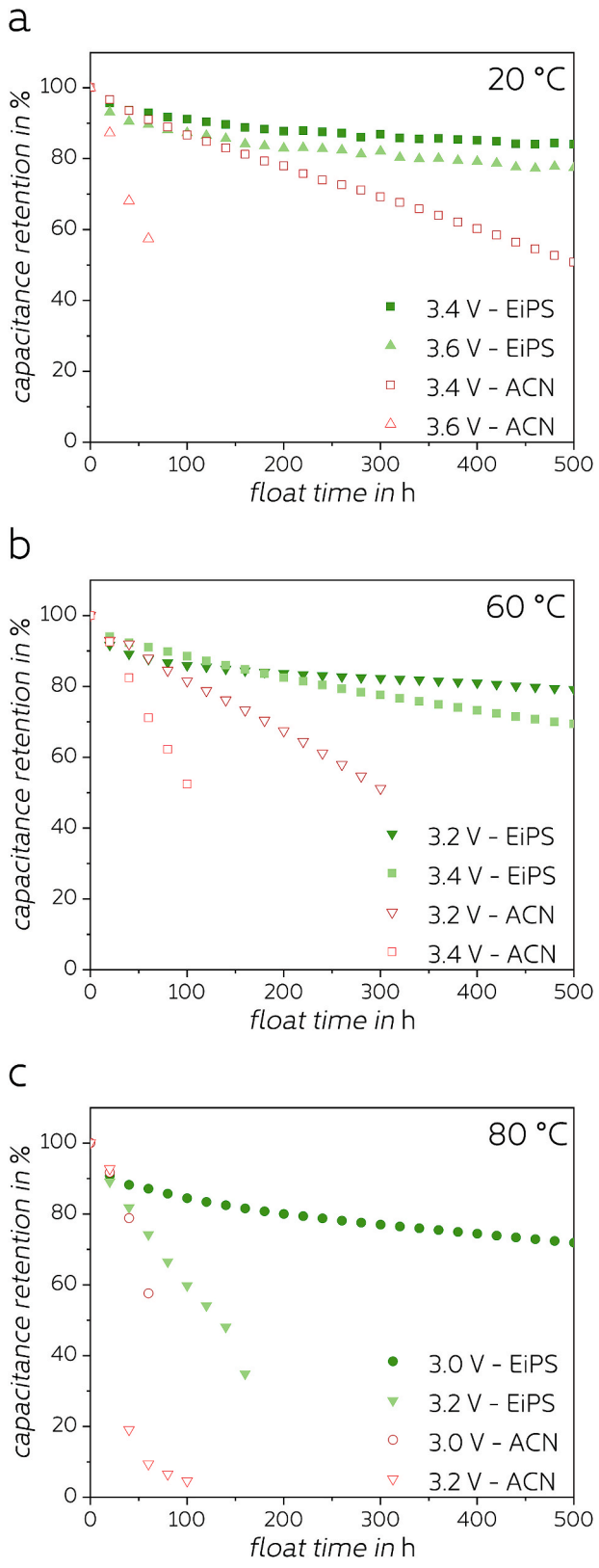

Fig. 7. Influence of different voltages on the capacitance retention in floating tests of 1 M $Pyr_{11}BF_4$ in EiPS and 1 M $Pyr_{11}BF_4$ in ACN at a) 20 °C, b) 60 °C, and c) 80 °C.

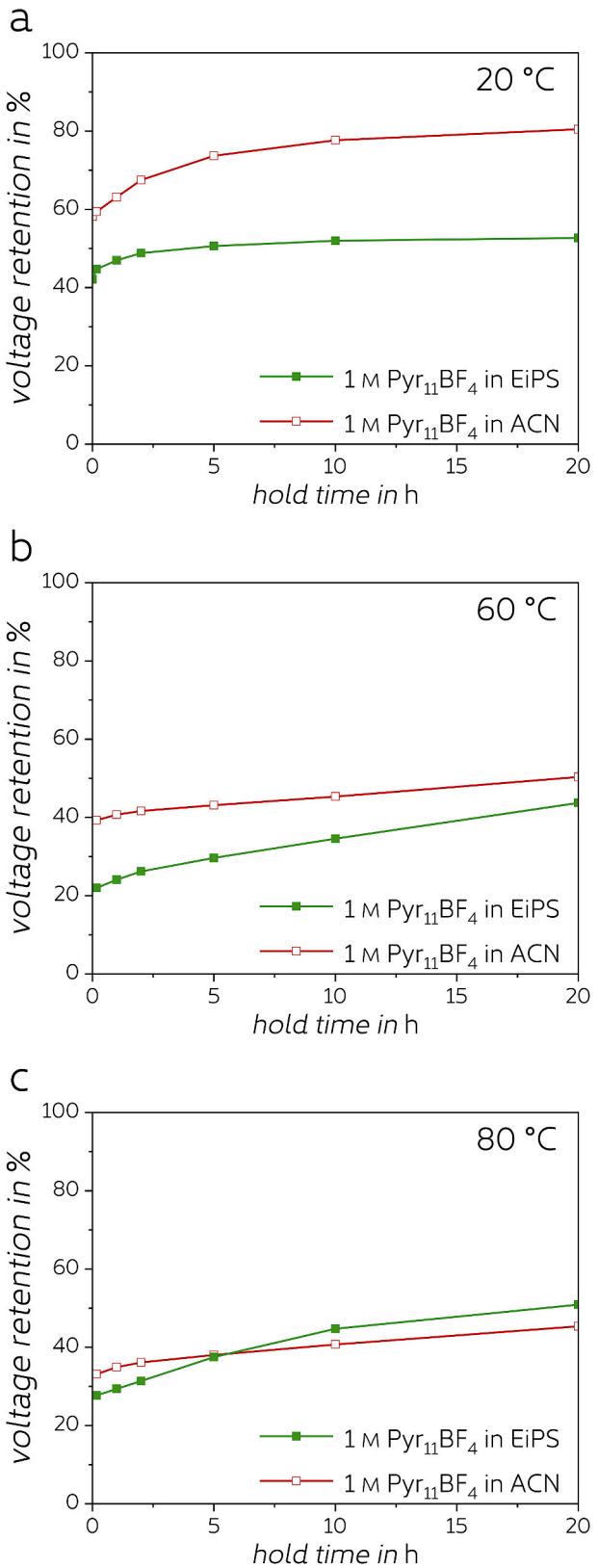

Fig. 8. Influence of the time holding the voltage constant at 3.0 V on the voltage retention of symmetrical EDLCs after self-discharging for 24 h. Self-discharge measurements were performed at a) 20 °C, b) 60 °C, and c) 80 °C with 1 M $Pyr_{11}BF_4$ in EiPS or ACN, respectively, as electrolytes.

EDLCs are known to have increased self-discharge due to faster ion transport [37,38]. This behavior can be observed for both devices at 60 °C (Fig. 8b). These accelerated self-discharge processes lead to higher voltage losses at a holding time of 10 min. While the EDLC based on ACN retains 39% of the initial voltage, the device based on EiPS can retain only 22%. However, when increasing the holding time at this temperature, the sulfone-based electrolytes benefit more from the longer holding time as both voltage retention curves approach each other. At the highest investigated temperature of 80 °C, the self-discharge increases further for the supercapacitor containing ACN leading to a voltage loss of 67% (Fig. 8c). Surprisingly, the EiPS-based EDLC is not losing further in voltage but less than at 60 °C. This might be connected to the formation of a passive layer, as described in a previous work for the electrolyte 0.5 M $TEABF_4$ in EiPS, which was attributed to the partial degradation of the solvent [32]. This faradic process was found to occur at temperatures of 60 °C or higher and voltage of 3.0 V or higher. Thus, the consumption of charges would lead to an additional faradic contribution to the self-discharge as long as the formation of the passivation layer is not complete. In fact, the voltage profiles for this electrolyte at 60 °C show an additional area with a different slope between the initial charge-redistribution at the beginning of the process and the gradual decrease due to ohmic leakage in the later part of the measurement (Fig. S4e in the SI). With elapsing time holding the voltage at 3.0 V, the faradic contribution disappears, leading to less self-discharge. Finally, the EiPS-based EDLC shows less self-discharge at a constant voltage holding time than the system based on ACN, represented by voltage retentions of 51% and 45%. Considering the EiPS' self-discharge behavior at higher temperatures, this solvent seems suitable for application in EDLCs in high-temperature surroundings when high stability and longevity of the energy storage device are desired.

4. Conclusion

Investigating the temperature-dependent behavior of alternative electrolytes based on EiPS and an ACN-based electrolyte as a reference gave interesting insights into the evolution of the electrochemical performance of EDLCs with increasing temperature. As electrolytes containing EiPS naturally have higher viscosity and lower ionic conductivity than the state-of-the-art ACN, EDLCs containing EiPS as the electrolyte solvent are limited in terms of high power capability and display higher internal cell resistance. We showed by temperature-dependent impedance spectroscopy that this resistance can be reduced by increasing the surrounding temperature. This improves the electrochemical performance at higher temperatures at the same time, as seen by temperature-dependent charge-discharge measurements. In contrast, electrolytes based on ACN lose performance with higher temperatures. This aligns EiPS- and ACN-based electrolytes at 80 °C, demonstrating the potential of EiPS for high-temperature applications. Especially due to the fact that EiPS-based EDLCs feature significantly higher stability against high voltage than ACN-based devices, as demonstrated by floating tests. This enables the operation of a symmetrical EDLC containing 1 M $Pyr_{11}BF_4$ in EiPS as electrolyte at a nominal voltage of 3.0 V and 80 °C while maintaining 72% of the initial capacitance after floating for 500 h. Lastly, the temperature significantly impacts the self-discharge behavior of EDLCs based on these solvents as well. While the conventional electrolyte displays less self-discharge at lower temperatures, the electrolyte based on EiPS improves with increasing temperature to show less self-discharge at 80 °C. Based on these results, the novel electrolyte formulation 1 M $Pyr_{11}BF_4$ in EiPS offers reduced internal cell resistance and improved electrochemical performance, especially at high temperatures and high rates compared to other electrolytes based on EiPS. Thus, it appears as an interesting electrolyte option for the development of high-temperature EDLCs that operate stably at high voltages. This could potentially offer a solution for applications in high-temperature surroundings in the future.

CRediT authorship contribution statement

Lukas Köps: carried out the experimental work reported in the manuscript and wrote the article draft. **Fabian Alexander Kreth:** carried out the experimental work reported in the manuscript and wrote the article draft. **Michel Klein:** carried out the experimental work reported in the manuscript and wrote the article draft. **Andrea Balducci:** wrote/finalized the article.

Declaration of competing interest

The authors declare that they have no known competing financial interests or personal relationships that could have appeared to influence the work reported in this paper.

Data availability

Data will be made available on request.

Acknowledgments

The authors would like to thank the Friedrich-Schiller-University Jena and the Bundesministerium für Wirtschaft und Klimaschutz (BMWK) within the project "SUPREME" (03EI6060B) for the financial support.

Appendix A. Supplementary data

Supplementary data to this article can be found online at https://doi.org/10.1016/j.jpowsour.2023.233480.

References

[1] A.F. Burke, J. Zhao, Past, present and future of electrochemical capacitors: technologies, performance and applications, J. Energy Storage 35 (2021), 102310, https://doi.org/10.1016/j.est.2021.102310.
[2] J.R. Miller, market and applications of electrochemical capacitors, in: F. Béguin, E. Frąckowiak (Eds.), Supercapacitors: Materials, Systems, and Applications, Wiley-VCH, Weinheim, 2013, pp. 509–526.
[3] T.P. Sumangala, M.S. Sreekanth, A. Rahaman, Applications of supercapacitors, in: K.K. Kar (Ed.), Handbook of Nanocomposite Supercapacitor Materials III, Springer International Publishing, Cham, 2021, pp. 367–393.
[4] K.V.G. Raghavendra, R. Vinoth, K. Zeb, C.V.V. Muralee Gopi, S. Sambasivam, M. R. Kummara, I.M. Obaidat, H.J. Kim, An intuitive review of supercapacitors with recent progress and novel device applications, J. Energy Storage 31 (2020), 101652, https://doi.org/10.1016/j.est.2020.101652.
[5] B. Babu, P. Simon, A. Balducci, Fast charging materials for high power applications, Adv. Energy Mater. 10 (2020), 2001128, https://doi.org/10.1002/aenm.202001128.
[6] R.S. Borges, A.L.M. Reddy, M.-T.F. Rodrigues, H. Gullapalli, K. Balakrishnan, G. G. Silva, P.M. Ajayan, Supercapacitor operating at 200 degrees celsius, Sci. Rep. 3 (2013), https://doi.org/10.1038/srep02572.
[7] R. Carter, A. Cruden, P.J. Hall, Optimizing for efficiency or battery life in a battery/supercapacitor electric vehicle, IEEE Trans. Veh. Technol. 61 (2012) 1526–1533, https://doi.org/10.1109/tvt.2012.2188551.
[8] L. Kouchachvili, W. Yaïci, E. Entchev, Hybrid battery/supercapacitor energy storage system for the electric vehicles, J. Power Sources 374 (2018) 237–248, https://doi.org/10.1016/j.jpowsour.2017.11.040.
[9] J.R. Miller, A. Burke, Electrochemical capacitors: challenges and opportunities for real-world applications, Electrochem. Soc. Interface 17 (2008) 53–57, https://doi.org/10.1149/2.f08081if.
[10] F. Beguin, V. Presser, A. Balducci, E. Frackowiak, Carbons and electrolytes for advanced supercapacitors, Adv. Mater. 26 (2014) 2219–2251, https://doi.org/10.1002/adma.201304137.
[11] K. Sharma Poonam, A. Arora, S.K. Tripathi, Review of supercapacitors: materials and devices, J. Energy Storage 21 (2019) 801–825, https://doi.org/10.1016/j.est.2019.01.010.
[12] H.V.T. Nguyen, J. Kim, K.-K. Lee, High-voltage and intrinsically safe supercapacitors based on a trimethyl phosphate electrolyte, J. Mater. Chem. 9 (2021) 20725–20736, https://doi.org/10.1039/d1ta05584d.
[13] A. Balducci, Electrolytes for high voltage electrochemical double layer capacitors: a perspective article, J. Power Sources 326 (2016) 534–540, https://doi.org/10.1016/j.jpowsour.2016.05.029.
[14] C. Schütter, S. Pohlmann, A. Balducci, Industrial requirements of materials for electrical double layer capacitors: impact on current and future applications, Adv. Energy Mater. 9 (2019), 1900334, https://doi.org/10.1002/aenm.201900334.

[15] A. Bothe, A. Balducci, Thermal analysis of electrical double layer capacitors: present status and remaining challenges, J. Power Sources 548 (2022), 232090, https://doi.org/10.1016/j.jpowsour.2022.232090.
[16] Z. Lin, E. Goikolea, A. Balducci, K. Naoi, P.L. Taberna, M. Salanne, G. Yushin, P. Simon, Materials for supercapacitors: when Li-ion battery power is not enough, Mater, Today Off. 21 (2018) 419–436, https://doi.org/10.1016/j.mattod.2018.01.035.
[17] R. Nigam, P. Sinha, K.K. Kar, Introduction to supercapacitors, in: K.K. Kar (Ed.), Handbook of Nanocomposite Supercapacitor Materials III, Springer International Publishing, Cham, 2021, pp. 1–38.
[18] M. Salanne, B. Rotenberg, K. Naoi, K. Kaneko, P.-L. Taberna, C.P. Grey, B. Dunn, P. Simon, Efficient storage mechanisms for building better supercapacitors, Nat. Energy 1 (2016), 16070, https://doi.org/10.1038/nenergy.2016.70.
[19] L.H. Hess, A. Bothe, A. Balducci, Design and use of a novel in situ simultaneous thermal analysis cell for an accurate "real time" monitoring of the heat and weight changes occurring in electrochemical capacitors, Energy Technol. 9 (2021), 2100329, https://doi.org/10.1002/ente.202100329.
[20] A. Bothe, A. Balducci, The impact of the thermal stability of non-conventional electrolytes on the behavior of high voltage electrochemical capacitors operating at 60 °C, Electrochim. Acta 374 (2021), 137919, https://doi.org/10.1016/j.electacta.2021.137919.
[21] A. Bothe, S.E.M. Pourhosseini, P. Ratajczak, F. Béguin, A. Balducci, Analysis of thermal and electrochemical properties of electrical double-layer capacitors by using an in-situ simultaneous thermal analysis cell, Electrochim. Acta 444 (2023), 141974, https://doi.org/10.1016/j.electacta.2023.141974.
[22] J. Krummacher, C. Schütter, L.H. Hess, A. Balducci, Non-aqueous electrolytes for electrochemical capacitors, Curr. Opin. Electrochem. 9 (2018) 64–69, https://doi.org/10.1016/j.coelec.2018.03.036.
[23] L. Köps, P. Ruschhaupt, C. Guhrenz, P. Schlee, S. Pohlmann, A. Varzi, S. Passerini, A. Balducci, Development of a high-energy electrical double-layer capacitor demonstrator with 5000 F in an industrial cell format, J. Power Sources 571 (2023), 233016, https://doi.org/10.1016/j.jpowsour.2023.233016.
[24] S. Pohlmann, Metrics and methods for moving from research to innovation in energy storage, Nat. Commun. 13 (2022), https://doi.org/10.1038/s41467-022-29257-w.
[25] J.R. Partington, E.G. Cowley, Dipole moment of acetonitrile, Nature 135 (1935), https://doi.org/10.1038/135474b0, 474-474.
[26] L.H. Hess, A. Balducci, 1,2-butylene carbonate as solvent for EDLCs, Electrochim. Acta 281 (2018) 437–444, https://doi.org/10.1016/j.electacta.2018.05.168.
[27] A. Krause, A. Balducci, High voltage electrochemical double layer capacitor containing mixtures of ionic liquids and organic carbonate as electrolytes, Electrochem. Commun. 13 (2011) 814–817, https://doi.org/10.1016/j.elecom.2011.05.010.
[28] A. Brandt, S. Pohlmann, A. Varzi, A. Balducci, S. Passerini, Ionic liquids in supercapacitors, MRS Bull. 38 (2013) 554–559, https://doi.org/10.1557/mrs.2013.151.
[29] T. Stettner, A. Balducci, Protic ionic liquids in energy storage devices: past, present and future perspective, Energy Storage Mater. 40 (2021) 402–414, https://doi.org/10.1016/j.ensm.2021.04.036.
[30] K. Chiba, T. Ueda, Y. Yamaguchi, Y. Oki, F. Shimodate, K. Naoi, Electrolyte systems for high withstand voltage and durability I. Linear sulfones for electric double-layer capacitors, J. Electrochem. Soc. 158 (2011) A872, https://doi.org/10.1149/1.3593001.
[31] C. Schütter, A. Bothe, A. Balducci, Mixtures of acetonitrile and ethyl isopropyl sulfone as electrolytes for electrochemical double layer capacitors, Electrochim. Acta 331 (2020), 135421, https://doi.org/10.1016/j.electacta.2019.135421.
[32] L. Köps, F.A. Kreth, D. Leistenschneider, K. Schutjajew, R. Gläßner, M. Oschatz, A. Balducci, Improving the stability of supercapacitors at high voltages and high temperatures by the implementation of ethyl isopropyl sulfone as electrolyte solvent, Adv. Energy Mater. 13 (2023), 2203821, https://doi.org/10.1002/aenm.202203821.
[33] H.V.T. Nguyen, K. Kwak, K.-K. Lee, 1,1-Dimethylpyrrolidinium tetrafluoroborate as novel salt for high-voltage electric double-layer capacitors, Electrochim, Acta 299 (2019) 98–106, https://doi.org/10.1016/j.electacta.2018.12.155.
[34] H.V.T. Nguyen, S. Lee, K. Kwak, K.-K. Lee, Bis(oxalate)borate-containing electrolytes for high voltage electric double-layer capacitors: a comparative study, Electrochim. Acta 321 (2019), 134649, https://doi.org/10.1016/j.electacta.2019.134649.
[35] L. Köps, F.A. Kreth, A. Bothe, A. Balducci, High voltage electrochemical capacitors operating at elevated temperature based on 1,1-dimethylpyrrolidinium tetrafluoroborate, Energy Storage Mater. 44 (2022) 66–72, https://doi.org/10.1016/j.ensm.2021.10.006.
[36] L.H. Hess, A. Balducci, Glyoxal-based solvents for electrochemical energy-storage devices, ChemSusChem 11 (2018) 1919–1926, https://doi.org/10.1002/cssc.201800375.
[37] B.W. Ricketts, C. Ton-That, Self-discharge of carbon-based supercapacitors with organic electrolytes, J. Power Sources 89 (2000) 64–69, https://doi.org/10.1016/S0378-7753(00)00387-6.
[38] H.A. Andreas, Self-discharge in electrochemical capacitors: a perspective article, J. Electrochem. Soc. 162 (2015) A5047–A5053, https://doi.org/10.1149/2.0081505jes.